Paper No.366/2021

INVESTIGATION OF THE REASON FOR THE DIFFERENCE IN THE ACOUSTIC LINER IMPEDANCE DETERMINED BY THE TRANSFER FUNCTION METHOD AND DEAN´S METHOD

[a)]Igor Khramtsov, [a)]Oleg Kustov, [a)]Vadim Palchikovskiy, [a)]Victor Ershov

[a)]Perm National Research Polytechnic University (PNRPU), Perm, Russia, lmgsh@pstu.ru

***Abstract**: The article considers the reason for the difference in the results of determining the impedance of the single-layer acoustic liner samples by different methods during the operation in a normal incidence impedance tube. The operation of the normal incidence impedance tube was simulated by numerical solution of the Navier-Stokes equations. The data obtained from the numerical simulation were processed by the transfer function method and Dean's method. A direct determination of the liner impedance, based on the ratio of the acoustic pressure to the acoustic normal velocity, was used to find out the reasons for the difference in impedance values. The analysis was carried out in the frequency range close to the resonance. It was shown that the transfer function method determines the impedance of the sample face, and the Dean's method determines the impedance of the one cell only.*

***Keywords:** Acoustic liner, normal incidence impedance tube, acoustic impedance, two-microphone transfer function method, Dean's method, numerical simulation*

***DOI:** 10.36336/akustika202139224*

1. INTRODUCTION

To reduce the noise of an aircraft engine, its ducts are treated with acoustic liners of the resonant type. These liners are cells of various shapes (honeycombs are commonly used), covered with perforated sheets. The fundamental characteristic of the liner is the acoustic impedance. This is a complex quantity that depends on the geometric parameters of the liner (porosity of sheet, depth of cells, thickness of the perforated sheet) and on specific external conditions (high sound pressure level, grazing flow in the duct). To predict the liner impedance one can use semi-empirical models, but the comparison of the predicted values with the results of the natural experiments on normal incidence impedance tubes (NIIT) shows that the discrepancy can be rather large [1-7].

In turn, the methods of experimental determination of the liner impedance also have some disadvantages. These methods are based on measurements with the microphones placed on the walls of the impedance tube or liner sample and give insufficient information about the processes occurring inside the sample. The placement of the measuring probes into the impedance tube or inside the liner sample, especially in the case of the multi-layer liners, leads inevitably to a distortion of the measured physical parameters. As a result, it is difficult to explain the difference in the impedance values obtained by various experimental methods and calculations [8-13].

For the reasons mentioned, the issue of liner impedance determination using numerical simulation has been actively studied for the last 20 years [14-24]. The numerical simulation is capable of more complete taking into account the entire range of physical processes accompanying the operation of the acoustic liner. This approach can be used both for direct simulation of a full-scale experiment on testing a liner sample and for determination of the physical quantities inside a sample, which can subsequently be used to refine impedance prediction models, as well as to correct the methods of experimental study of an acoustic liner.

Previously, the authors proposed a technique based on numerical simulation of processes in NIIT, which allows predicting the acoustic characteristics of the single-, double-, and triple-layer resonant liners at high sound pressure levels (SPL) [21-24]. For better compliance of the calculation procedure with the full-scale experiment, the results of the numerical simulation in the technique were processed by the two-microphone transfer function method [25].

Another way to determine the acoustic characteristics of the liner samples is the Dean's method [26]. Its adaptation to numerical simulation was previously carried out by the authors for the case of normal incidence of waves [11], as well as for the case of grazing incidence of waves [27]. At the same time, a difference was found in the acoustic characteristics when they were determined by the Dean's method and by the transfer function method at the normal incidence of a sound wave [11].

In this work, the study continues to compare the methods for determining the acoustic characteristics of the liner samples. As a result of the work, the new data on the spatial and spectral structure of the sound field inside the liner, which are problematic to extract in full-scale experiment, were obtained. Based on the data obtained, it is possible to find an impedance directly from the ratio of the acoustic pressure to the acoustic velocity, and thereby to verify the methods involved in determining the impedance.

2. METHODS INVOLVED IN DETERMINING IMPEDANCE

As is known, the normalized impedance is defined as the ratio of the acoustic pressure $\boldsymbol{p}$ at a point on the liner face to the acoustic velocity $\boldsymbol{u_n}$ normal to the liner at the same point:

$$\boldsymbol{Z} = \frac{\boldsymbol{p}}{\boldsymbol{u_n}} \frac{\boldsymbol{1}}{\boldsymbol{\rho c}} \tag{1}$$

where
$\boldsymbol{\rho}$ is a density of a medium,
$\boldsymbol{c}$ is a sound speed.

However, in practice, finding the impedance directly from the formula (1) is problematic due to the difficulties in the simultaneous measurement of acoustic parameters at a point directly on the face of the liner sample. In this regard, various microphone methods are used to determine the acoustic characteristics of the liner samples.

The simplest way for determining acoustic characteristics is to conduct the measurements of the liner sample on NIIT and to process obtained data by the transfer function method (hereinafter TFM) [25, 28]. This method is based on measuring the pressure at two points in NIIT duct at a small distance from the face of the sample (usually 1-1.5 duct diameter), where only a plane wave propagates. The reflection coefficient is determined from the measured transfer function $\boldsymbol{H_{21}}$ between the two microphones:

$$\boldsymbol{R} = \frac{\boldsymbol{H_{21}} - \boldsymbol{e^{-ik(l_2 - l_1)}}}{\boldsymbol{e^{ik(l_2 - l_1)}} - \boldsymbol{H_{21}}} \cdot \boldsymbol{e^{2ikl_2}}. \tag{2}$$

Here
$\boldsymbol{k}$ is a spatial wave number,
$\boldsymbol{l_1}$ is a distance from a liner sample to the first microphone,
$\boldsymbol{l_2}$ is a distance from a liner sample to the second microphone,
$\boldsymbol{i}$ is an imaginary unit.

Based on the reflection coefficient obtained in (2), we can further calculate the normalized acoustic impedance:

$$\boldsymbol{Z} = \frac{\boldsymbol{1+R}}{\boldsymbol{1-R}}. \tag{3}$$

In [26], another two-microphone method for determining the impedance was proposed, where the acoustic pressure on the face of the liner sample and on the back wall of the sample is measured. Commonly it is called the in-situ method, but hereinafter we call it the Dean's method (DM). An important advantage of this method is that it can be used to determine the acoustic characteristics not only at the normal incidence of an acoustic wave, but also to be used to study the properties of the liner directly on an aircraft engine [9]. The normalized acoustic impedance in terms of the acoustic pressure at the liner face and the back wall is determined as:

$$\boldsymbol{Z} = -\boldsymbol{i} \frac{\boldsymbol{P_{face-sheet}}}{\boldsymbol{P_{back-wall}}} \boldsymbol{e^{i\varphi}} \boldsymbol{sin^{-1}(kh)}, \tag{4}$$

where
$\boldsymbol{h}$ is a liner depth,
$\boldsymbol{\varphi}$ is a phase angle between the face sheet acoustic pressure and the back wall acoustic pressure.

3. SPECIFICS OF THE NUMERICAL SIMULATION

The article considers two liner samples. The first sample is a single Helmholtz resonator with one orifice in the center (Fig. 1a). The second sample is a single-layer sample (Fig. 1b) with geometrics close to the liner used for real aircraft engines. This sample consists of seven cells of a honeycomb shape. The wall thickness between honeycombs is 1 mm. There are 5 orifices per honeycomb. The characteristics of the samples in detail are presented in Tab. 1. The acoustic impedance of these samples was previously obtained through measurements on NIIT and processing the experimental data by TFM. The impedance of the samples was also determined based on numerical simulations. Comparison of the experiment and the computation demonstrates a good correspondence of obtained impedance. A detailed description of the experiments and numerical simulation are presented in [21, 29].

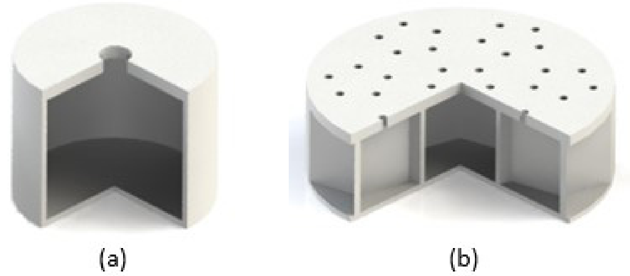

Fig. 1: The samples under consideration: (a) model sample; (b) sample H14D50

Обозначение	Thickness of the perforated plate [mm]	Height [mm]	Orifice diameter [mm]	External diameter of a sample D_e [mm]	Inner diameter of a sample D_i, [mm]
Model sample	2	20	5	30	28
H14D50	2	14	1,5	50	35

Tab. 1: Characteristics of the liner samples

In this work, the acoustic characteristics of the samples were determined based on the solution of a nonstationary gas dynamic problem, since this is the only way to take into account the physical effects proper to the liner operation at high SPL [24]. The numerical simulation of acoustic processes in NIIT was carried out by a direct numerical solution of the compressible Navier-Stokes equations in three-dimensional formulation. The computations were performed in the laminar statement in the ANSYS Fluent.

The computational domain is a part of NIIT duct with a length of 120 mm and an internal volume of the corresponding sample. Fig. 2 shows a general view of the computational domains, boundary conditions, and points that simulate microphones. A boundary condition "Wall" was used on the walls of NIITs and the samples. At the entrance to the computational domain, the boundary condition "Outlet" was used:

$$p|_{S_1} = P_{rand}(t)$$

$$T|_{S_1} = 300K$$

were

$P_{rand}(t)$ is a time function with a uniform frequency spectrum in the given frequency range of 500-3600 Hz.

The signa level at the entrance to the computational domain was selected so as to provide a total SPL on the sample face of about 140 dB. At each time step of computation, the values at the "Outlet" boundary were updated from the ''pressure-time" file recorded previously in a full-scale experiment. As a result, a plane wave propagated inside the computational domain, similar in spectral composition to the sound signal generated in a natural experiment on NIIT. The sound waves reflected from the sample left the computational domain through the section S1 (Fig. 2).

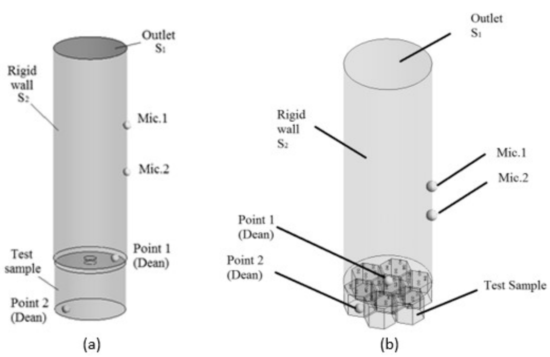

Fig. 2: Computational domain: (a) model sample; (b) sample H14D50

The density was determined by the given pressure and temperature from the equation of state for an ideal gas. It was used a pressure-based coupled solver, an implicit time difference scheme of the second-order accuracy, and numerical schemes of the second-order accuracy in spatial variables to approximate convective terms in the equations.

To save computational resources, the CutCell mesh was used. The mesh was thickened in the area of the resonator neck in such a way that there were 15-20 elements on throat height. Additionally, thickening at the wall of 15 layers with a growth factor of 1.2 is used. The depth of the wall layer was 0.002 mm. The linear dimensions of the element increase as the distance from the neck increases until the average linear dimension reaches 2 mm. The part of the computational mesh is presented in Fig. 3.

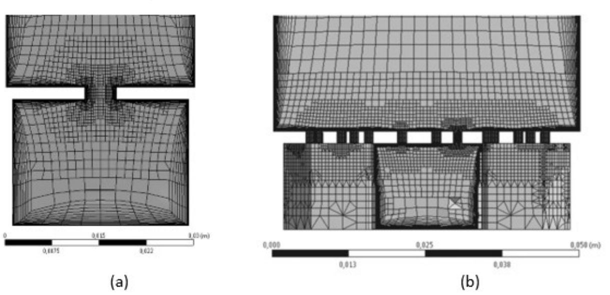

Fig. 3: Computational mesh: (a) model sample (400 000 elements); (b) sample H14D50 (2 200 000 elements)

The computations were carried out with a time step of 1/65536 s. The number of time steps was 332768. This made it possible to construct spectra with a step of 2 Hz. At each time step, the following signals were recorded: static pressure at Mic. 1, Mic. 2, Point 1, Point 2 (Fig. 3); static pressure averaged over the sample face; normal velocity averaged over the sample face, over the orifices, over the free cross-sectional area inside the sample. The recorded signals were split into segments, every segment was multiplied by the Hanning window and processed by the fast Fourier transform, and the spectra were averaged over the number of the signal segments. Averaging was carried out with an overlap of 66%.

4. ANALYSIS OF THE RESULTS

The data recorded in the numerical simulation at Mic. 1 and Mic. 2 points (Fig. 3) were processed by TFM according to formulas (2), (3). The data recorded at Point 1 and Point 2 (Fig. 3) were processed by DM according to formula (4). In addition, the determination of the impedance by a direct calculation (hereinafter referred to as the DC) according to the expression (1) was implemented, since numerical simulation, in contrast to a natural experiment, makes it possible to obtain pressure and normal velocity signals at any point within the liner sample.

At the first stage, to determine the impedance of the model sample, the values of pressure and normal velocity averaged over the sample face were used. As you can see in Fig. 4, all methods give close values in the resonant frequency region. With a distance of more than 200 Hz from the resonant frequency, all methods differ from each other; this is especially true for the real part of the impedance Re(Z) obtained by TFM. However, we focus on the analysis in the region near the resonant frequency. It is seen that the values Re(Z) obtained by DM are slightly less than those obtained by TFM and DC.

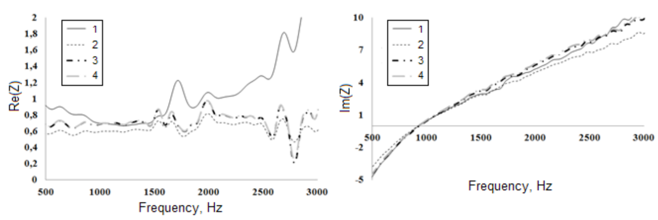

Fig. 4: Comparison of the model sample impedance: 1 – TFM; 2 – DM; 3 – DC, with averaging pressure and normal velocity over the sample face; 4 – DC, pressure is taken at a point on the sample face, the normal velocity is averaged over the sample face

If the impedance is considered as a uniformly distributed value on the sample face, then the pressure and velocity averaged over the sample face should be used. However, it is not possible to determine the pressure distributed over the sample face in full-scale experiment. Assuming that only a plane wave propagates in NIIT, the pressure is determined at a point on the sample face using a microphone. At the same time, numerical simulation allowed us to obtain both data at points and data averaged over the sample face. The pressure spectra in several points on the sample face were compared with each other and with the spectrum averaged over the sample face (Fig. 5). As you can see, the pressure spectra at different points are very close; hence, the impedance determined from the pressures at these points is almost the same. This is confirmed in Fig. 4, curve 4 almost completely coincides with curve 3, therefore, the impedance can be determined using the pressure at a point and the average velocity over the sample face.

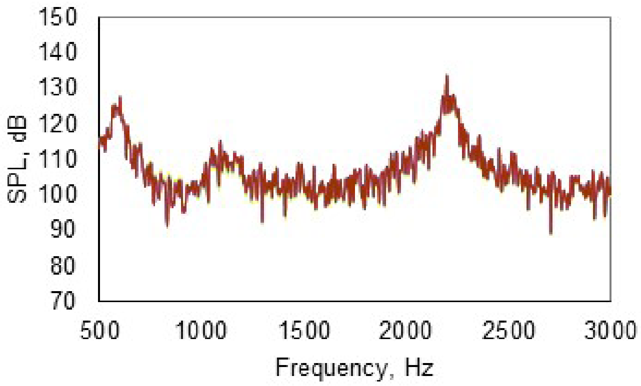

Fig. 5: Spectra of the pressure at four different points on the sample face and pressure averaged over the sample face

As the normal velocity on the wall is zero, only the normal velocity in the orifices of the perforated plate contributes to the velocity averaged over the sample face. The mass flow rate is a constant, therefore only a porosity of a perforated plate is required to be taken into account for correction of the velocity. As this takes place, the question arises, how to determine the porosity? The mass flow generated by the acoustic driver in NIIT propagates through the duct and then passes through the orifices. Accordingly, to correct the velocity, the porosity can be determined by the ratio of the area of the orifice to the area of the sample face ($\boldsymbol{S_e}$). The flow that has passed through the orifice in the perforated plate continues to propagate inside the sample. Therefore, it is possible to determine the porosity through the ratio of the total area of the orifices to the free cross-sectional area inside the sample ($\boldsymbol{S_i}$). Usually, it is considered that there is no difference between these values of the porosity and it is calculated from the area of the sample face. However, for the model sample, the porosity, defined as $\boldsymbol{F_e=S_{orifice}/S_e}$, is 0.026. If we define the porosity as $\boldsymbol{F_e=S_{orifice}/S_i}$, then it becomes equal to 0.032. Let us compare the contributions of these quantities to the impedance. For this case, formula (1) is written as:

$$Z = \frac{p}{Fu_{orifice}}\frac{1}{\rho c} \tag{5}$$

where

$\boldsymbol{F}$ is a porosity of a face plate,

$\boldsymbol{u_{orifice}}$ is a normal velocity in an orifice.

As can be seen in Fig. 4 and Fig. 6, the impedance determined by DC with porosity $\boldsymbol{F_e}$ (Fig. 6, curve 3) coincides with the impedance determined by DC, using the values of pressure and normal velocity averaged over the sample face (Fig. 4, curve 3). In this case, these values in the region of the resonant frequency of the sample coincide with TFM (Fig. 4, curve 1 and Fig. 6, curve 1). The impedance determined by DC according to formula (5) with the use of porosity $\boldsymbol{F_i}$ (Fig. 6, curve 4), coincides with DM (Fig. 4, curve 2 and Fig. 6, curve 2). In this regard, it can be concluded that TFM determines the impedance of the sample face and DM determines the impedance of the one cell only.

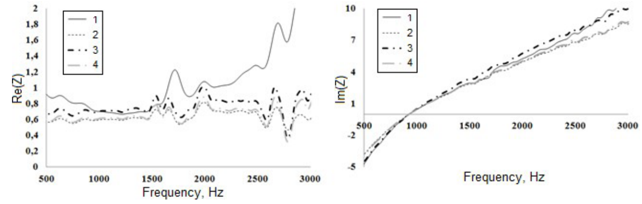

Fig. 6: Comparison of the impedance for the model sample: 1 – TFM; 2 — DM; 3 — DC, pressure is taken at a point, normal velocity is averaged over $S_{orifice}$, porosity F_e is used; 4 — DC, pressure is taken at a point, normal velocity is averaged over $S_{orifice}$, porosity F_i is used

Since in the model sample the whole internal volume is occupied by only one cell, then to check the conclusion made above, the impedance for sample H14D50, which already consists of 7 cells, was determined by similar calculations. Fig. 7 shows a comparison of the impedance determined by different methods. For this sample, similarly, the impedance obtained by TFM and DM are different in the region of the resonant frequency. The porosity for the sample defined as $\boldsymbol{F_e=\Sigma S_{orifice}/S_e}$ is 0.032. If the porosity is determined based on the free cross-sectional area of the sample, then due to the presence of walls between the honeycombs, the porosity is equal to 0.042 ($\boldsymbol{F_i=\Sigma S_{orifice}/S_i}$). It is seen, that in the resonant frequency region of the sample, the impedance determined by TFM is the same as the impedance determined by DC for the porosity $\boldsymbol{F_e}$, and the impedance determined by MD is the same as the impedance determined by the DC for the porosity $\boldsymbol{F_i}$.

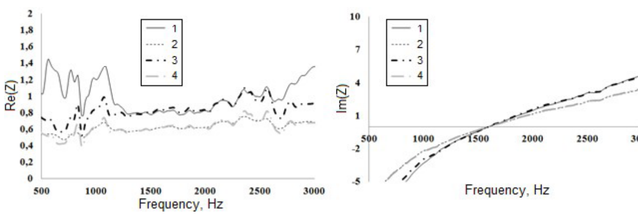

Fig. 7: Comparison of the impedance for sample H14D50: 1 – TFM; 2 — DM; 3 — DC, pressure is taken at a point, normal velocity is averaged over total $S_{orifice}$, porosity F_e is used; 4 — DC, pressure is taken at a point, normal velocity is averaged over total $S_{orifice}$, porosity F_i is used

5. CONCLUSION

The work considered the determination of the acoustic impedance using different methods for two single-layer liner samples. The impedance of the samples was determined by the transfer function method (TFM) and the Dean's method (DM) based on data obtained in the numerical simulation of the physical processes in a normal incidence impedance tube. Comparison of the impedance values revealed their difference. To explain this result, the impedance was also determined by a direct calculation (DC) – from the ratio of the acoustic pressure to the normal acoustic velocity on the sample face. The use of the pressure and the normal velocity averaged over the sample face yielded the impedance close to that determined by TFM.

Then, it was shown that to determine the impedance, one can use the pressure at a point on the sample face and the normal velocity averaged over the orifices, but in so doing the porosity of the sample should be taken into account. Besides, the porosity can be determined from both the area of the sample face (porosity $\boldsymbol{F_e}$) and from the free cross-sectional area inside the sample (porosity $\boldsymbol{F_i}$). For the samples under consideration, the porosity, determined by these methods, differs by 0.01 due to the presence of walls between the cells.

As a result, a comparison of the impedance obtained using different methods revealed that: in the region of the resonant frequency of the sample, the impedance determined by TFM coincides with the impedance determined by DC using the porosity $\boldsymbol{F_e}$; impedance determined by DM coincides with the impedance determined by DC using the porosity $\boldsymbol{F_i}$. In this regard, it can be concluded that TFM determines the impedance of the sample face and DM determines the impedance of the one cell only.

ACKNOWLEDGEMENT

The work was funded by a grant from the President of the Russian Federation for young scientists - candidates of science MK-541.2021.1.2.

REFERENCES

[1] Ingard, U.: Absorption characteristics of nonlinear acoustic resonators, Journal of the Acoustical Society of America, Vol. 44, No. 4, p. 1155-1156, 1968
[2] Melling, T.H.: The acoustic impedance of perforates at mediumand high sound pressure levels, Journal of Sound and Vibrations, Vol. 29, No. 1, p. 1-65, 1973
[3] Guess, A.W.: Calculation of perforated plate liner parameters from specified acoustic resistance and reactance, Journal of Sound and Vibrations, Vol. 40, No. 1, p. 119-137, 1975
[4] Ingard, U.: On the theory and design of acoustic resonators, Journal of the Acoustical Society of America, Vol. 25, No. 6, p. 1037-1061, 1953
[5] Stinson, M.R., Shaw, E.A.: Acoustic impedance of small, circular orifices in thin plates, Journal of the Acoustical Society of America, Vol. 77, No. 6, p. 2039-2042, 1985
[6] Elnady, T., Boden, H.: On the modeling of the acoustic impedance of perforates with flow, AIAA Paper, No. 3304, 2003
[7] Khramtsov, I.V., Kustov, O.Yu., Palchikovskiy, V.V., Bulbovich, R.V.: Comparison of acoustic characteristics of resonant liner samples at normal incidence of waves based on semiempirical model, natural experiment and numerical simulation, AIP Conference Proceeding, to be published
[8] Motsinger, R.E., Kraft, R.E.: Design and performance of duct acoustic treatment, Aeroacoustics of flight vehicles. Theory and practice, Acoustical Society of America, New York, 1995
[9] Gaeta, R.J., Mendoza, J.M., Jones, M.G.: Implementation of in-situ impedance techniques on a full scale aero-engine system, AIAA Paper, No. 2007-3441, 2007
[10] Schuster B.: A comparison of ensemble averaging methods using Dean's method for in-situ impedance measurements, AIAA Paper, No. 2012-2244, 2012
[11] Khramtsov, I.V., Kustov, O.Y., Palchikovskiy, V.V.: Adaptation of the Dean method to determine the acoustic characteristics of liner samples based on numerical simulation of physical processes in a normal incidence impedance tube, 2020 International Conference on Dynamics and Vibroacoustics of Machines, DVM 2020, 2020
[12] Bodén, H., Cordioli, J.A., Spillere, A., Serrano P.: Comparison of the effect of flow direction on liner impedance using different measurement methods, AIAA Paper, No. 2017-3184, 2017
[13] Sobolev, A.F., Ostrikov, N.N., Anoshkin, A.N., Palchikovskiy, V.V., Burdakov, R.V., Ipatov, M.S., Ostroumov, M.N., Yakovets, M.A.: Comparison of liner impedance derived from the results of measurements at two different setups using a small number of microphones, PNRPU Aerospace Engineering Bulletin, No. 45, p. 59-113, 2016
[14] Fedotov, E.S., Palchikovskiy, V.V.: A study of Helmholtz resonator operation in rectangular cross-section waveguide, PNRPU Aerospace Engineering Bulletin, No. 38, p. 107-126, 2014
[15] Komkin, A.I., Mironov, M.A., Yudin, S.I.: Eigenfrequency of a Helmholtz resonator at the wall of a rectangular duct, Acoustical Physics, Vol. 60, No. 2, p. 145-151, 2014
[16] Na, W., Boij, S., Efraimsson, G.: Simulations of acoustic wave propagation in an impedance tube using a frequency-domain linearized Navier-Stokes solver, AIAA Paper, No. 2014-2960, 2014
[17] Gély, D., Elias, G., Lupoglazoff, N., Vuillot, F., Micheli, F.: Aeroacoustics characterization and numerical simulation of a Helmholtz resonator, AIAA Paper, No. 99-1941, 1999
[18] Tam, C.K.W., Kurbatskii, K.A., Ahuja, K.K., Gaeta, J.R.: A numerical and experimental investigation of the dissipation mechanisms of resonant acoustic liners, Journal of Sound and Vibration, Vol. 245, No. 3, p. 545-557, 2001
[19] Tam, C.K.W., Ju, H., Jones, M.G., Watson, W.R., Parott, T.L.: A computational and experimental study of slit resonators, Journal of Sound and Vibration, Vol. 284, p. 947-984, 2005

[20] Roche, J.M., Leylekian, L., Delattre, G., Vuillot, F.: Aircraft fan noise absorption: DNS of the acoustic dissipation of resonant liners, AIAA Paper, No. 3146, 2009
[21] Khramtsov, I.V., Kustov, O.Yu., Fedotov, E.S., Siner, A.A.: On numerical simulation of sound damping mechanisms in the cell of a sound-absorbing structure, Acoustical Physics, Vol. 64, No. 4, p. 511-517, 2018
[22] Khramtsov, I.V., Kustov, O.Yu., Palchikovskiy, V.V.: Determination of acoustic characteristics of full-scale sample of single-layered honeycomb liner based on numerical simulation, Akustika, Vol. 32, p. 182-188, 2019
[23] Khramtsov, I.V., Kustov, O.Yu., Palchikovskiy, V.V.: Determination of acoustic characteristics of the double-layer honeycomb liner based on numerical simulation, Akustika, Vol. 34, p. 32-36, 2019
[24] Khramtsov, I.V., Kustov, O.Yu., Fedotov, E.S., Siner, A.A.: On numerical simulation of sound damping mechanisms in the cell of a sound-absorbing structure, Acoustical Physics, Vol. 64, No. 4, p. 511-517, 2018
[25] Chung, J.Y., Blaser, D.A.: Transfer function method of measuring in-duct acoustic properties. I. Theory. II. Experiment, Journal of the Acoustical Society of America, Vol. 68, No. 3, p. 907-921, 1980
[26] Dean P. D. An in-situ method of wall acoustic impedance measurement in flow duct, Journal of Sound and Vibration, Vol. 34, No. 1, pp. 97-103, 1974
[27] Khramtsov, I.V., Kustov, O.Y., Palchikovskiy: Technique for evaluating the acoustic properties of a liner at grazing incidence of wave based on numerical simulation, AIP Conference Proceedings, to be published
[28] ISO 10534-2, Acoustics – Determination of sound absorption coefficient and impedance in impedance tubes – Part 2: Transfer-function method
[29] Fedotov, E.S., Khramtsov, I.V., Kustov, O.Y.: Numerical simulation of the processes in the normal incidence tube for high acoustic pressure levels, AIP Conference Proceedings, Vol. 1770, No. 030120, 2016

Igor Khramtsov *is Ph.D. of Engineering Science, researcher of the Laboratory of Noise Generation Mechanisms and Modal Analysis, and Assistant Professor of the Perm National Research Polytechnic University. His research area includes aeroacoustics, investigation of characteristics of sound-absorbing structures and materials, and acoustic measurements. He presented the main results of scientific research at the international conferences in Moscow, St. Petersburg, Novosibirsk, and Perm.*

Oleg Kustov *is junior researcher of the Laboratory of Noise Generation Mechanisms and Modal Analysis, and postgraduate student of the Perm National Research Polytechnic University. His research area includes acoustic measurements, and investigation of characteristics of sound-absorbing structures and materials. He presented the main results of scientific research at the international conferences in Moscow, Kazan, Novosibirsk, and Perm.*

Vadim Palchikovskiy *is Ph.D. of Engineering Science, researcher of the Laboratory of Noise Generation Mechanisms and Modal Analysis, and Associate Professor of the Perm National Research Polytechnic University. His research area includes acoustic measurements, investigation of characteristics of sound-absorbing structures and materials, numerical methods and programming, numerical simulation of acoustic processes. He presented the main results of scientific research at the international conferences in Moscow, St. Petersburg, Kazan, and Perm.*

Victor Ershov *is junior researcher of the Laboratory of Noise Generation Mechanisms and Modal Analysis, and postgraduate student of the Perm National Research Polytechnic University. His research area includes acoustic measurements, and numerical methods and programming. He presented the main results of scientific research at the international conferences in Moscow, Novosibirsk, and Perm.*